Published in final edited form as:
AJR Am J Roentgenol. 2014 August ; 203(2): 329–335. doi:10.2214/AJR.13.11811.

Adrenal incidentaloma triage with single source (fast kVp switch) dual energy CT

Daniel I Glazer, MD,
University of Michigan Radiology, UH B1D502, 1500 E Medical Ctr Dr, Ann Arbor, MI 48109, Phone (734) 615-4924, Fax (734) 763-9523

Nahid R Keshavarzi, MS,
Michigan Institute for Clinical and Health Research, Biostatistics Core, 2800 Plymouth Rd, Bldg 400, Ann Arbor, MI 48109, Phone (734) 998-7474, Fax (734) 998-7228

Katherine E Maturen, MD,
University of Michigan Radiology, UH B1D530, 1500 E Medical Ctr Dr, Ann Arbor, MI 48109, Phone (734) 232-6004, Fax (734) 615-1276

Robert A Parker, ScD,
Michigan Institute for Clinical and Health Research, Biostatistics Core, 2800 Plymouth Rd, Bldg 400, Ann Arbor, MI 48109, Phone (734) 998-7474, Fax (734) 998-7228

Ravi K Kaza, MD,
University of Michigan Radiology, UH B1D502, 1500 E Medical Ctr Dr, Ann Arbor, MI 48109, Phone (734) 763-4051, Fax (734) 763-9523

Joel F Platt, MD, and
University of Michigan Radiology, UH B1D540, 1500 E Medical Ctr Dr, Ann Arbor, MI 48109, Phone (734) 936-4462, Fax (734) 615-1276

Isaac R Francis, MD
University of Michigan Radiology, UH B1D540, 1500 E Medical Ctr Dr, Ann Arbor, MI 48109, Phone (734) 936-4488, Fax (734) 615-1276

Daniel I Glazer: glazerd@umich.edu; Nahid R Keshavarzi: nahidk@umich.edu; Katherine E Maturen: kmaturen@umich.edu; Robert A Parker: robert.a.parker.scd@gmail.com; Ravi K Kaza: ravikaza@umich.edu; Joel F Platt: jplatt@umich.edu; Isaac R Francis: ifrancis@umich.edu

Abstract

Purpose—To evaluate single source dual energy CT (DECT) for distinguishing benign and indeterminate adrenal nodules, with attention to effects of phase of intravenous contrast enhancement.

Materials and methods—An IRB-approved, HIPAA-compliant retrospective review revealed 273 contrast-enhanced abdominal DECTs from November 2009–March 2012. 50 adrenal nodules ≥ 0.8 cm were identified in 41 patients: 22 female, 19 male, average age 66 (range 36–88 years). CT post-processing and measurements were independently performed by two radiologists (R1 and

Correspondence to: Katherine E Maturen, kmaturen@umich.edu.

R2) for each nodule: (1) HU on true non-contrast images; (2) post-contrast HU on monochromatic spectral images at 40, 75, and 140 keV; (3) post-contrast material density (mg/cc) on virtual non-contrast (VNC) images. Nodules were separated into benign (<10 HU) and indeterminate (≥ 10 HU) based on true non-contrast images.

Results—Interreader agreement regarding benign and indeterminate nodules was high (kappa 0.92, 95% CI 0.8–1.0). At 140 keV, HU of benign nodules was significantly lower (Reader 1: 6.9 HU ±13.9; Reader 2: 7.1 HU ±10.7) than indeterminate nodules (R1: 17.5 HU ±18.1 (*p* .003); R2: 21.3 HU ±10.9 (*p* <.0001) at 65–120 seconds after contrast injection. In VNC images, benign nodules had significantly lower material density (R1: 992.4 mg/cc ± 9.9; R2: 992.7 mg/cc ±9.6) than indeterminate nodules (R1: 1001.1mg/cc ±20.5 (*p* .038); R2: 1007.6 HU ±13.4 (*p* <.0001).

Conclusion—DECT tools can mathematically subtract iodine or minimize its effects in high energy reconstructions, approximating non-contrast imaging and potentially reducing the need for additional studies to triage adrenal nodules detected on post-contrast DECT exams.

INTRODUCTION

Adrenal nodules are a common unexpected finding present in at least 4% ocf the imaged general population [1, 2]. Although they are overwhelmingly likely to be benign in a patient without cancer history [3], such nodules are often incompletely characterized by single phase contrast-enhanced CT exams. Nodules detected during routine contrast-enhanced CT exams are generally evaluated with either chemical shift MR or a follow-up non-contrast CT, the latter enabling distinction of benign fat-containing lesions such as lipid-rich adenoma and myelolipoma with attenuation < 10 HU from indeterminate nodules with attenuation ≥ 10 HU [4, 5]. Indeterminate nodules can be further characterized with contrast-enhanced CT using a 15 minute delay and calculation of percent washout [6–8]. The ability to classify a lesion as either benign or indeterminate on single-phase contrast-enhanced CT could potentially save the patient a second and even a third CT acquisition--reducing both medical costs and individual patient radiation dose.

As dual energy CT (DECT) becomes increasingly common in clinical practice [9], incidental adrenal masses will be detected and require characterization. Fortunately, this technology has unique capabilities that may obviate the need for additional imaging. Several recent papers have evaluated the utility of DECT in the characterization of adrenal nodules, all using a dual source DECT platform. Investigators have focused on two specific tools in DECT: virtual monochromatic spectral (VMS) images and virtual non-contrast (VNC) images [10–12]. VMS images can be retrospectively generated at any energy level to approximate a CT acquisition at that tube potential. Although most tissue types exhibit lower CT numbers at higher CT tube potentials, fat increases in CT number at higher kVp. Thus, because of their adipose content, lipid rich adenomas evaluated with non-contrast CT have been shown to exhibit higher CT numbers in VMS images at higher reconstructed energy levels [13], but this effect has not been assessed on contrast-enhanced CT images. Second,, strong correlation has been reported between nodule attenuation measurements in iodine-subtracted virtual non-contrast (VNC) images vs. true non-contrast images [10–12]. Although iodine subtraction efficacy may vary with iodine density, this work has not generally evaluated the effect of phase of enhancement on this correlation. Further, these

features have only been reported using dual source DECT, and have not been assessed on the single source (fast kVp switch) DECT platform.

The relationship between CT number and iodine density on post contrast DECT images is linear and positive [14], but has some complexity: the degree of correlation is higher for more intensely enhancing vessels and organs and declines progressively in less-enhancing structures [15]. Thus, we hypothesize that the density of iodine within an adrenal nodule could affect both nodule attenuation at various energy levels and efficacy of iodine subtraction techniques. Adrenal nodules are incidentally discovered on studies performed for various indications, with a variety of bolus timing protocols. If a specific DECT tool is to be broadly applied for problem solving in such cases, the relevant phases of enhancement must be specified. The purpose of this study is to evaluate single source (fast kVp switch) DECT for adrenal mass triage and characterization, including VMS reconstructions at various energy levels and VNC imaging, with attention to the effects of phase of contrast enhancement.

METHODS

Patients

With Institutional Review Board approval, reports of imaging studies were retrospectively reviewed from 273 consecutive contrast-enhanced DECT abdomen exams for any indication between November 2009 and March 2012, identified via the radiology information system (Imagecast, GE Healthcare) using the “GSI” search term included by dictating radiologists and a review of CT logs for the relevant scanners. 64 patients whose dictated radiology reports described an adrenal nodule and who had a concurrent or prior true non-contrast CT were further evaluated by consensus review of their CT images. Nodules that were not clearly visible or did not meet reference standards specified below were excluded. 50 nodules ≥ 0.8 cm in size were identified in 41 patients: 22 female and 19 male, average age 66 (range 36–88 years). Mean body mass index was 30.0 (range 18.9–49.6), overweight by current CDC guidelines [16]. 38 patients underwent CT protocols that included a concurrent non-contrast acquisition and 3 had prior non-contrast CTs 24, 13, and 11 months prior to the DECT respectively, which were used for comparison. Prior imaging studies were reviewed as needed for reference standard in lesion characterization.

CT technique

DECT exams were initially performed for a variety of indications with several different protocols, including CTA prior to (n=2) or after (n=14) endovascular aneurysm repair (EVAR), renal (n=11) or adrenal (n=9) mass evaluation, CT urogram (n=2), and abdomen/pelvis CT (n=3). Thus, intravenous contrast quantity, rate of injection, and bolus timing varied (Table 1). Patients underwent DECT scanning using a GE HD-750 scanner equipped with fast switch-kVp (single source) dual energy technology (GE Healthcare, Milwaukee WI), where the tube voltage rapidly switches between 80 and 140 kVp. Based on the patient size and weight, one of the available Gemstone Spectral Imaging (GSI) presets was chosen; these vary in tube current, gantry rotation time and scan field of view, and hence have varying weighted CT Dose Index (CTDIw) values. Pitch and slice thickness varied with

protocol, but 2.5 mm slices were used for subsequent material density and attenuation measurements. True non-contrast imaging was performed with standard single energy technique (helical scanning with 2.5 mm slice thickness at 120 kVp, automated tube current with minimum 100 mA/maximum 575 mA, pitch 1.375:1), whether done as part of the DECT exam or during a separate imaging session. Non contrast (single energy) series had a mean dose-length product (DLP) 278.1 mGy-cm (SD 106.1, range 97.7–486.2) while post contrast (dual energy) series had a mean DLP 575.4 mGy-cm (SD 177.3, range 277.5–1122.8).

Lesion Analysis

All DECT datasets were post-processed using commercially available software on a dedicated workstation using Gemstone Spectral Imaging (GSI) software (GE Advantage Workstation versions 4.5 and 4.6, GE Healthcare, Milwaukee WI). Independent sets of measurements were made by two radiologists, one a senior radiology resident and the other an abdominal radiologist with 5 years of post-fellowship experience. The same radiologists had previously reviewed the cases for inclusion, so they were not blinded, but clinical and non-study imaging information was not used during research measurement sessions. First, lesion attenuation was measured on standard true non-contrast images on the axial image where the lesion appeared largest, using a single region of interest (ROI) as large as possible but entirely within each nodule. The entire nodule was encompassed and areas of heterogeneity were included within ROIs, to make the method as reproducible as possible. Second, using contrast-enhanced DECT datasets, virtual monochromatic spectral (VMS) images were created at various energy levels (Figure 1) and ROIs placed similarly. Third, material density analysis was performed using a workstation preset two-material decomposition to generate virtual non-contrast (VNC) or “iodine-subtracted” datasets using the (iodine:water) material density basis pair and ROIs again placed within lesions. VNC images do not give HU information but rather material density in mg/cc iodine on the GE DECT platform. The following data were thus recorded for each nodule: 1) HU on true non-contrast images, 2) HU on reconstructed VMS images at 40, 75, and 140 keV, and 3) material density (mg/cc) on reconstructed VNC images.

Reference Standards

The 0.8 cm nodule size was selected based on the recognition that the diameter of the body of the normal adrenal gland rarely exceeds 0.6 cm or the limbs 0.3 cm [17], and that modern multidetector scanners readily demonstrate adrenal nodules as small as 0.5 cm [18]. Long axis nodule measurements were performed on axial images. A nodule was considered benign (lipid-rich adenoma, cyst or myelolipoma) if it had true non-contrast attenuation < 10 HU (n=30), and indeterminate (lipid-poor adenoma and other) if it measured ≥ 10 HU (n=20) on non-contrast CT [4, 19]. Lipid-rich adenomas had true non-contrast attenuation < 10 HU (n=28) and/or were surgically confirmed (n=1), while nodules containing macroscopic fat with stable size > 2 years were considered myelolipomas (n=1). Nodules that measured ≥ 10 HU on non-contrast CT were considered (lipid-poor) adenomas if they underwent confirmatory biopsy (n=1), demonstrated washout > 60% on 15 minute delayed contrast-enhanced CT (n=6), opposed phase signal loss on chemical shift MR imaging (n=3), or were stable in size for > 2 years with non-contrast attenuation 10–30 HU (n=8).

Indeterminate nodules that decreased in size on follow-up imaging and exhibited blooming on long-TE MR imaging were considered hematomas (n=2).

Statistical Analysis

For purposes of statistical analysis, phases of enhancement were grouped (Table 1). Kappa statistics were used to determine the consistency between readers of the classification of benign vs. indeterminate lesions. Variability in the difference between readers' HU levels was assessed using linear regression. Wilcoxon rank sum test was used to assess differences in lesion attenuation at the various keV levels for benign (<10 HU) and indeterminate (≥10 HU) lesions, and for the difference in material density. Mixed models ANOVA was performed to assess differences between phases of contrast enhancement. Pearson coefficients were used to assess correlation between true non-contrast (HU) and virtual non-contrast (mg/cc) measurements. Logistic regression was used for Receiver Operating Characteristic (ROC) analysis; comparisons between ROC curves were done using the DeLong, DeLong and Clarke-Pearson procedure. All statistical procedures were performed with SAS Version 9.3 software (SAS Institute, Inc., Cary, NC).

RESULTS

Nodules

Among 50 nodules, average diameter was 2.1 cm (range 0.8–7.2 cm). 8 patients had bilateral nodules; among the remaining 33 patients there were 27 left sided nodules and 7 right sided. (One patient had two discrete left sided nodules.) Final diagnosis based on pathologic specimens (n=2) and imaging features detailed above (n=48) included 47 adenomas (29 lipid-rich and 18 lipid-poor), 2 adrenal hemorrhages, and 1 myelolipoma. Because of the variety of scan indications and protocols, some nodules were imaged in only one phase of enhancement post contrast, while others were imaged up to three times (Table 1). 23 nodules were scanned in the early phase, 44 in the middle phase, and 7 in the late phase according to this grouping.

Reader consistency

Interreader agreement regarding true non-contrast lesion attenuation, the key variable separating lesions into "benign" and "indeterminate" groups, was high (kappa 0.92, 95% CI 0.8–1.0). However, the difference between HU measurements by the two readers is not constant. Differences between the two readers' measurements decreased as the CT number of the lesion decreased (p .0088) but did not significantly change with size of mass (p .35). When lesion attenuation in HU was measured at various keV levels (virtual monochromatic series), no significant difference was noted between readers at 40 keV in any phase of enhancement. At 75 keV, the usual reconstruction used for clinical interpretation, differences between readers were inversely correlated with lesion size (p .0008). At 140 keV, differences between readers were inversely correlated with lesion attenuation (p .0003) and marginally with lesion size (p .08), but there was no significant relationship with phase of enhancement.

Virtual monochromatic spectral (VMS) images

Regarding lesion characterization using virtual monochromatic spectral (VMS) images benign and indeterminate nodules did not differ significantly in attenuation at 40 or 75 keV, or in attenuation change between 40 to 140 keV during any phase (Wilcoxon Rank sum test; all $p > 0.05$). All had lower CT numbers at higher reconstructed energy levels, in all phases of enhancement. However, HU differed significantly ($p < .01$) between the two lesion groups at 140 keV (Table 2, Figure 2),, both in the middle phase of enhancement and when all phases of enhancement are combined (). Because the readers differed in their group assignment of two lesions by TNC HU measurements, each reader's lesion classification was tested separately.

Virtual non-contrast (VNC) images

Finally, regarding lesion characterization by virtual non-contrast images, there was a strong positive correlation between true non-contrast (TNC in HU) and virtual non-contrast (VNC in mg/cc) measurements for both readers, which was most robust in the middle phase of enhancement (Reader 1: 0.42, p .004; Reader 2: 0.66, p <.0001) and when all phases are combined (Reader 1: 0.43, p .0001; Reader 2: 0.54, p <.0001). Material density measurements of benign and indeterminate nodules were significantly different in the middle phases of enhancement (Table 3).

Finally, direct comparison of diagnostic performance (Figures 3 and 4) for detecting indeterminate nodules by VMS imaging at 140 keV vs. iodine subtracted VNC imaging did not reveal significant differences between the two tests, for either reader.

DISCUSSION

Using single source DECT, this study demonstrates that benign and indeterminate adrenal nodules differ significantly in both mean attenuation (HU) in virtual monochromatic spectral (VMS) images at 140 keV and material density (mg/cc) in virtual non-contrast (VNC) images using the iodine:water basis pair. Differences are most pronounced in the middle phases of enhancement, which included acquisitions at 65–120 seconds after contrast injection (Table 1). All 50 nodules, including 29 lipid-rich adenomas and a myelolipoma, decreased in CT number at numerically higher reconstructed monochromatic energy levels.

In standard non-contrast CT imaging, the lipid content of adrenal nodules is a major driver of attenuation and provides much of the foundation for current management recommendations in adrenal mass imaging. The present study illustrates two methods of approximating non-contrast imaging, using DECT techniques, from contrast-enhanced images. Both methods minimize the effects of iodinated contrast, by either maximizing the distance from iodine's k-edge, or mathematically subtracting iodine via a two-material decomposition algorithm, respectively. The composition of adrenal nodules can potentially be unmasked by either technique, such that intracellular lipid is no longer obscured by the dominant imaging effects of iodine.

One prior DECT study evaluating adrenal nodule attenuation at various tube potentials was limited to non-contrast imaging [13]. The authors found that some lipid-rich adenomas

exhibited diminished CT numbers in 80 kVp CT acquisitions compared with 140 kVp, or otherwise stated, that the lipid content of these masses led to increased CT number at higher tube potentials. This has not been confirmed by other investigators using contrast enhanced DECT. We too observed the opposite effect, likely because the effect of iodine (which rapidly decreases in CT number as tube potential or reconstructed energy level increases) outweighs that of lipid (which has a more gradual rate of decrease in CT number at increased energies).

We found that the CT numbers of benign and indeterminate nodules differed significantly in VMS images reconstructed at 140 keV. Although a similar result with single source (fast kVp switch) DECT has been presented in scientific sessions [20], to our knowledge it has not been previously published. Most investigators have used dual source DECT, where an analogous reconstruction is not possible. A reconstructed monochromatic series at 75 keV approximates a 120 kVp acquisition [21], because the effective monoenergetic level of a polychromatic 120 kVp CT beam is 70–75 keV. A 140 keV reconstructed monochromatic series is purely synthetic and does not have an analogous true scanner setting, as the setting would have to be above the maximum available setting of 140 kVp on most scanners. Using single source DECT, the monochromatic VMS images are synthesized from the concentrations of specified basis pair materials (such as iodine and water) using the known mass x-ray attenuation coefficients of these materials at various energy levels. At 40 keV, the effects of iodine are vastly overemphasized because the mass attenuation coefficient of iodine is about three orders of magnitude greater than that of water, while at 140 keV the mass attenuation coefficients of water and iodine are very similar [14, 22]. The effects of iodinated contrast are minimized by maximizing the energy distance from the k-absorption edge of iodine (33.2 keV), and the changes in HU with increasing iodine concentration are known to be minimal at this very high reconstructed energy level (140 keV) [14]. Thus, this effect was observed during all phases of enhancement.

We found that material density of benign and indeterminate nodules differed significantly in VNC images. Our findings are concordant with prior studies regarding the utility of VNC imaging [10, 11], but vary slightly from recently published conclusions regarding delayed phase timing in DECT for adrenal nodules [12]. The authors concluded that sensitivity for adenoma detection in VNC images from dual source DECT was impaired by technical failure of iodine subtraction, a problem that was more marked in the portal venous phase than the 15-minute delayed phase [12]. Technical differences between the material decomposition algorithms employed by single source and dual source DECT systems suggest that virtual non-contrast imaging on different vendor platforms may not be strictly equivalent [14, 23, 24]. However, it is logical that incomplete iodine subtraction would be more problematic in the portal venous than delayed phase due to the known substantial de-enhancement (and relative absence of iodinated contrast) of most adenomas in the latter phase [6–8]. The small number of delayed phase observations in our study compared with other phases may have obscured this phenomenon. Finally, it should be noted that iodine subtraction efficacy varies with body habitus [25] and the mean body mass index was in the overweight to obese range in our patient population. Thus, although such demographics could be encountered in many North American hospitals, our results may not be entirely typical of a “normal weight” population.

The clinical significance of these findings is that patients with incidentally detected adrenal nodules on contrast-enhanced DECT of the abdomen may be able to avoid additional imaging studies for nodule characterization. The unique capabilities of DECT to mathematically subtract iodine or minimize its effects can approximate non-contrast imaging and potentially spare patients additional time, anxiety, expense, and radiation exposure. The existing literature does not support a specific role for DECT as a primary modality for characterization of adrenal nodules identified by other imaging studies.

This retrospective study is limited by the number and histologic variety of adrenal nodules analyzed. We did not have any malignant nodules to support a subgroup analysis. The standard of reference (benign vs. indeterminate nodules using the 10 HU threshold) is itself an imaging test, and the study would be improved by inclusion of a greater number of pathologically proven lesions. This is a frequent limitation in adrenal imaging studies, given the preponderance of benign lesions for which no intervention is indicated. Inter-reader reliability diminished with lesion size and at 140 keV, likely both a result of decreased nodule conspicuity and greater difficulty in placing ROIs. Despite these variations, the same trends and relationships were noted in both readers' data, suggesting that the effects are robust enough to be recreated by readers with slightly varying measurement techniques and experience. Finally, readers were not blinded to VMS results when performing VNC measurements and vice versa, because readers sequentially performed each step in DECT post-processing during reading sessions.

In summary, our study is the first to our knowledge to evaluate single source DECT for adrenal incidentaloma triage, and demonstrates significant differences between benign and indeterminate adrenal nodules on both virtual monochromatic spectral (VMS) images at 140 keV and virtual non-contrast (VNC) images derived from contrast-enhanced single source (fast kVp switch) DECT. These technologies approximate true non-contrast imaging and potentially obviate the need for additional imaging in patients with incidentally detected adrenal nodules on contrast-enhanced DECT exams performed between 65 to 120 seconds after contrast administration. 140 keV VMS and VNC imaging performed similarly to each other in all phases of enhancement in this study. Favoring its simplicity for users, we suggest that investigation of DECT for adrenal nodules should continue to focus on VNC imaging, with the goal of standardizing single source DECT VNC data in mg/cc and dual source DECT VNC data in HU to establish a broadly applicable quantitative threshold for benignity.

Acknowledgments

The authors gratefully acknowledge Mitchell Goodsitt, PhD for assistance with manuscript review.

References

1. Kloos RT, Gross MD, Francis IR, Korobkin M, Shapiro B. Incidentally discovered adrenal masses. Endocr Rev. 1995; 16:460–484. [PubMed: 8521790]
2. Bovio S, Cataldi A, Reimondo G, et al. Prevalence of adrenal incidentaloma in a contemporary computerized tomography series. J Endocrinol Invest. 2006; 29:298–302. [PubMed: 16699294]

3. Song JH, Chaudhry FS, Mayo-Smith WW. The incidental adrenal mass on CT: prevalence of adrenal disease in 1,049 consecutive adrenal masses in patients with no known malignancy. AJR Am J Roentgenol. 2008; 190:1163–1168. [PubMed: 18430826]
4. Boland GW, Lee MJ, Gazelle GS, Halpern EF, McNicholas MM, Mueller PR. Characterization of adrenal masses using unenhanced CT: an analysis of the CT literature. AJR Am J Roentgenol. 1998; 171:201–204. [PubMed: 9648789]
5. Berland LL, Silverman SG, Gore RM, et al. Managing incidental findings on abdominal CT: white paper of the ACR incidental findings committee. J Am Coll Radiol. 2010; 7:754–773. [PubMed: 20889105]
6. Caoili EM, Korobkin M, Francis IR, et al. Adrenal masses: characterization with combined unenhanced and delayed enhanced CT. Radiology. 2002; 222:629–633. [PubMed: 11867777]
7. Pena CS, Boland GW, Hahn PF, Lee MJ, Mueller PR. Characterization of indeterminate (lipid-poor) adrenal masses: use of washout characteristics at contrast-enhanced CT. Radiology. 2000; 217:798–802. [PubMed: 11110946]
8. Park BK, Kim CK, Kim B, Lee JH. Comparison of delayed enhanced CT and chemical shift MR for evaluating hyperattenuating incidental adrenal masses. Radiology. 2007; 243:760–765. [PubMed: 17517932]
9. Megibow AJ, Sahani D. Best practice: implementation and use of abdominal dual-energy CT in routine patient care. AJR Am J Roentgenol. 2012; 199:S71–77. [PubMed: 23097170]
10. Gnannt R, Fischer M, Goetti R, Karlo C, Leschka S, Alkadhi H. Dual-energy CT for characterization of the incidental adrenal mass: preliminary observations. AJR Am J Roentgenol. 2012; 198:138–144. [PubMed: 22194489]
11. Ho LM, Marin D, Neville AM, et al. Characterization of adrenal nodules with dual-energy CT: can virtual unenhanced attenuation values replace true unenhanced attenuation values? AJR Am J Roentgenol. 2012; 198:840–845. [PubMed: 22451549]
12. Kim YK, Park BK, Kim CK, Park SY. Adenoma characterization: adrenal protocol with dual-energy CT. Radiology. 2013; 267:155–163. [PubMed: 23329655]
13. Gupta RT, Ho LM, Marin D, Boll DT, Barnhart HX, Nelson RC. Dual-energy CT for characterization of adrenal nodules: initial experience. AJR Am J Roentgenol. 2010; 194:1479–1483. [PubMed: 20489086]
14. Zhang D, Li X, Liu B. Objective characterization of GE discovery CT750 HD scanner: gemstone spectral imaging mode. Med Phys. 2011; 38:1178–1188. [PubMed: 21520830]
15. Kaza, RK.; Maturen, KE.; Al Hawary, MM.; Pandya, A.; Wasnik, AP.; Platt, JF. Dual energy CT in the abdomen: Correlation between post-contrast iodine density and degree of enhancement. Abstract presented at Radiological Society of North America annual meeting; Chicago, IL. 2012.
16. CDC. Body Mass Index: Considerations for Practitioners. Department of Health and Human Services: Centers for Disease Control and Prevention; http://www.cdc.gov/obesity/downloads/BMIforPactitioners.pdf [accessed 7/25/13]
17. Vincent JM. The size of normal adrenal glands on computed tomography. Clinical radiology. 1994; 49:453–455. [PubMed: 8088036]
18. Whitley SA. The appearance of the adrenal glands on computed tomography in multiple endocrine neoplasia type 1. European journal of endocrinology. 2008; 159:819–824. [PubMed: 18827064]
19. Lee MJ, Hahn PF, Papanicolaou N, et al. Benign and malignant adrenal masses: CT distinction with attenuation coefficients, size, and observer analysis. Radiology. 1991; 179:415–418. [PubMed: 2014283]
20. Land, A.; Morgan, D.; Weber, T.; Fineberg, N.; Lockhart, M. Adrenal Gland Material Density Analysis Utilizing Dual Energy Spectral MDCT: Intrapatient Comparison With Conventional Unenhanced MDCT. Abstract presented at American Roentgen Ray Society annual meeting; Chicago, IL. 2011.
21. Zou, Y.; Silver, MD. Analysis of fast kV-switching in dual energy CT using a pre-reconstruction decomposition technique. In: Hsieh, J.; ES, editors. SPIE. 2008.
22. Goodsitt MM, Christodoulou EG, Larson SC. Accuracies of the synthesized monochromatic CT numbers and effective atomic numbers obtained with a rapid kVp switching dual energy CT scanner. Med Phys. 2011; 38:2222–2232. [PubMed: 21626956]

23. Kaza RK, Platt JF, Cohan RH, Caoili EM, Al-Hawary MM, Wasnik A. Dual-energy CT with single- and dual-source scanners: current applications in evaluating the genitourinary tract. Radiographics. 2012; 32:353–369. [PubMed: 22411937]

24. Toepker M, Moritz T, Krauss B, et al. Virtual non-contrast in second-generation, dual-energy computed tomography: reliability of attenuation values. Eur J Radiol. 2012; 81:e398–405. [PubMed: 22236702]

25. Miller CM. Effect of organ enhancement and habitus on estimation of unenhanced attenuation at contrast-enhanced dual-energy MDCT: concepts for individualized and organ-specific spectral iodine subtraction strategies. American journal of roentgenology (1976). 2011; 196:W558–564.

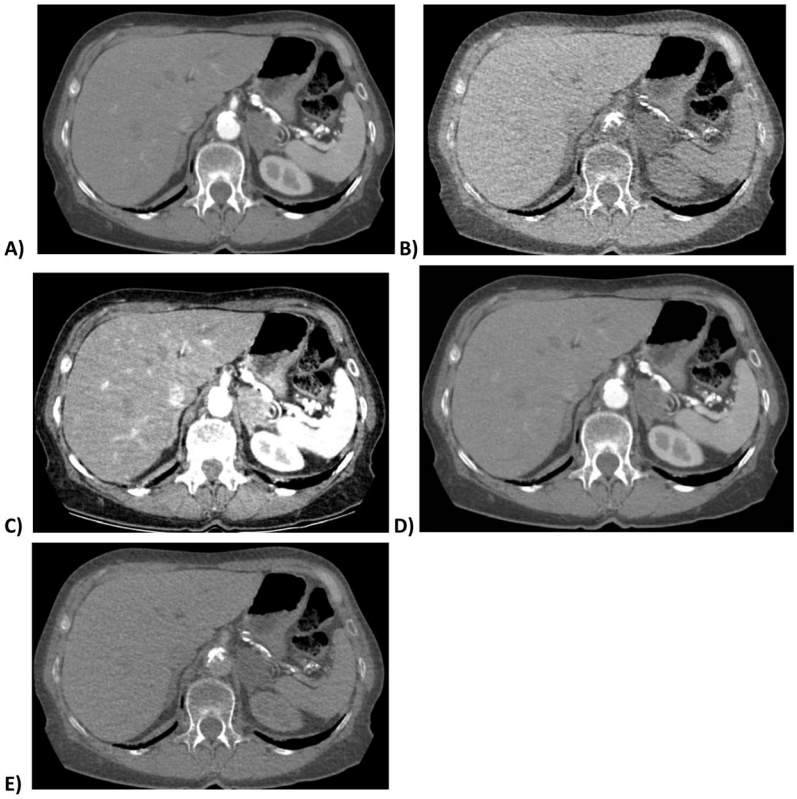

Figure 1. 70 year old woman with lipid-rich left adrenal adenoma

DECT images show the nodule in the arterial phase of enhancement (A) and a virtual non-contrast (VNC) image (B) derived from the same series using the iodine:water material basis pair. Calcium in the aorta remains in image B after iodine subtraction. Images C–E are virtual monochromatic spectral (VMS) images at 40, 75 and 140 keV, respectively. Note the decreasing conspicuity of iodine at higher reconstructed monochromatic energy levels. E is similar but not identical to B, with E exhibiting persistent subtle corticomedullary differentiation and less noise.

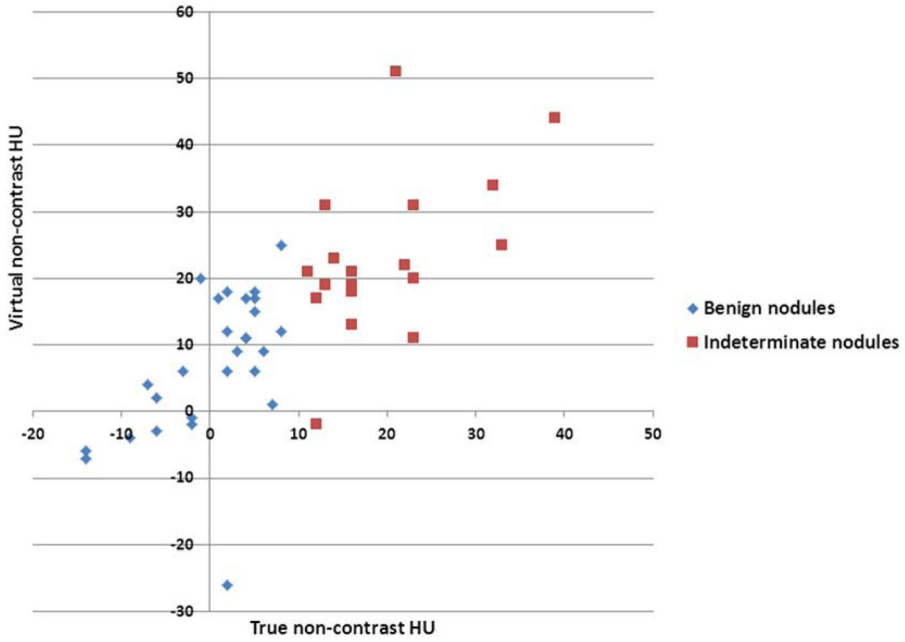

Figure 2.

Scatter plot of benign and indeterminate nodules showing Hounsfield unit (HU) measurements of nodules in 140 keV virtual monochromatic spectral images reconstructed from DECT data at 65–120 seconds after contrast administration.

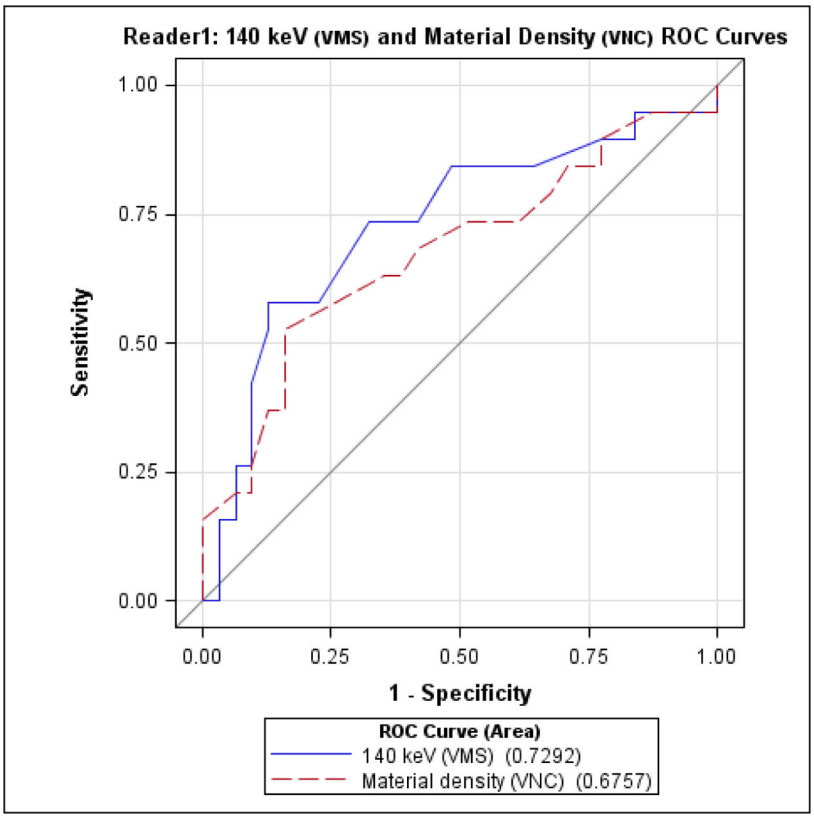

Figure 3.

Reader 1 receiver-operator characteristics for detecting indeterminate nodules, comparing virtual monochromatic spectral (VMS) imaging at 140 keV and material density measurements from virtual non-contrast (VNC) images.

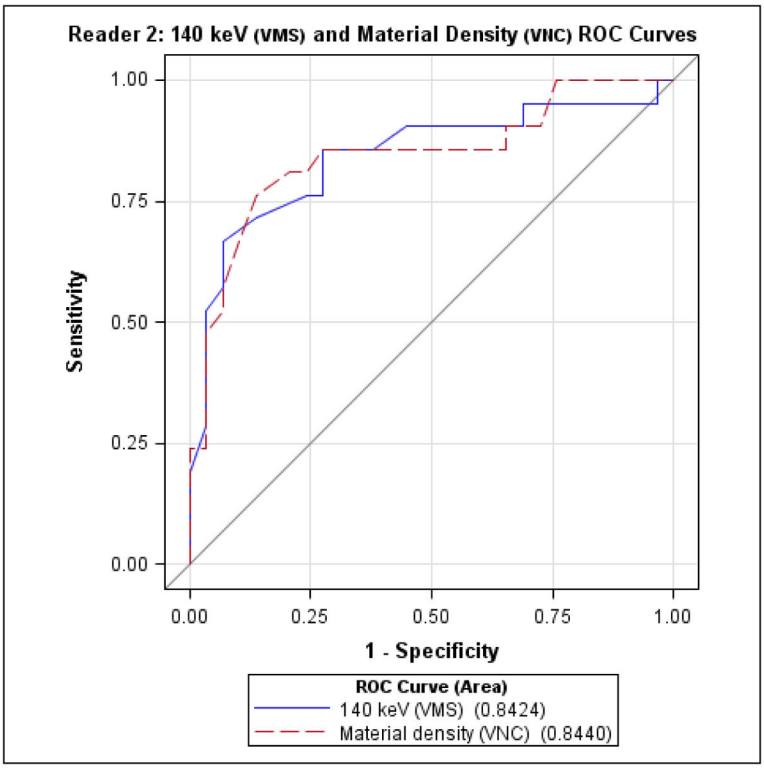

Figure 4.

Reader 2 receiver-operator characteristics for detecting indeterminate nodules, comparing virtual monochromatic spectral (VMS) imaging at 140 keV and material density measurements from virtual non-contrast (VNC) images.

Table 1

Bolus timing for designated enhancement groups.

Phase of enhancement	Time in seconds after start of bolus injection	Group	Protocols including the specified phase
Arterial	~35	Early	• Aorta • Renal mass post ablation
Portal venous	65	Middle	• Abdomen/pelvis • Adrenal mass
Venous delay	~90		• Post-endograft aorta
Nephrographic	120		• Renal mass • Renal mass post ablation
Excretory	600	Late	• CT urogram • Renal mass post ablation
Adrenal mass protocol delay	900		• Adrenal mass

Table 2

Virtual monochromatic spectral (VMS) images: mean nodule attenuation values in HU (SD).

Reconstructed keV level	Reader	Middle phases only (n= 44)		*p*	All nodules in all phases combined (n =74)		*p*
		Benign (< 10 HU) R1 n=29, R2 n=27	Indet. (≥ 10 HU) R1 n=15, R2 n=17		Benign (< 10 HU) R1 n=50, R2 n=48	Indet. (≥ 10 HU) R1 n=24, R2 n=26	
140 keV	R1	6.9(13.9)	17.5(18.1)	***.003***	7.0(12.5)	15.7(20.5)	***.004***
	R2	7.1(10.7)	21.3(10.9)	***<.0001***	7.8(9.2)	17.5(13.4)	***<.0001***

Table 3

Virtual non-contrast (VNC) images: mean material density measurements of nodules in mg/cc (SD). NS= not statistically significant.

Reader	Early phase (n= 23)		*p*	Middle phases (n= 44)		*p*	Late phases (n =7)		*p*
	Benign (< 10 HU) R1/R2 n=17	**Indet. (≥ 10 HU) R1/R2 n=6**		**Benign (< 10 HU) R1 n=29, R2 n=27**	**Indet. (≥ 10 HU) R1 n=15, R2 n=17**		**Benign (< 10 HU) R1/R2 n= 4**	**Indet. (≥ 10 HU) R1/R2 n=3**	
R1	993.2(7.7)	996.7(9.6)	NS	992.4(9.9)	1001.1(20.5)	***.038***	996.5(4)	1004(30.8)	NS
R2	996.6(5.8)	1003.5(12.2)	NS	992.7(9.6)	1007.6(13.4)	***<.0001***	998(1.4)	994.3(23.7)	NS